Charge Separation in Donor-Chromophore-Acceptor Complexes: Inverted Region Behavior in Reverse Electron Transfer Reactions

S. L. Larson, L. F. Cooley,† C. M. Elliott,* and D. F. Kelley*

Contribution from the Department of Chemistry, Colorado State University, Fort Collins, Colorado 80523. *Received February 3, 1992. Revised Manuscript Received May 26, 1992*

Abstract: Time-resolved absorption studies which elucidate intramolecular electron transfer rates have been performed on a series of covalently linked Ru(bipyridine)$_3$-donor-acceptor complexes. In these complexes the electron donor is a phenothiazine moiety linked to a bipyridine by a $(-CH_2-)_4$ chain, and the electron acceptor is an *N,N'*-diquaternary-2,2'-bipyridinium moiety, linked to a bipyridine by a $(-CH_2-)_2$ chain. Excitation to the Ru(bipyridine)$_3$ metal-to-ligand charge transfer (MLCT) state leads to a long-lived charge-separated state which is shown to form by oxidative quenching of the $Ru(bpy)_3^{2+}$ moiety followed by phenothiazine-to-ruthenium electron transfer. A wavelength dependent excitation into a charge transfer state results in very rapid formation of the charge-separated state. The magnitude of the fast component in the transient absorption serves as an internal standard for determining reverse electron transfer rates as a function of the energetic driving force. Marcus inverted behavior is observed and analyzed in terms of high frequency electron acceptor vibrations.

Introduction

Chromophore-quencher complexes which act as photoinduced charge transfer systems have been extensively studied due to their ability to store optical energy in the form of charge-separated states. Most charge-separation schemes utilize intermolecular electron transfer (ET), but systems in which chromophores and quenchers are covalently attached have recently received considerable attention.[1] While the majority are made up of a chromophore and either an electron acceptor or an electron donor, there are a few examples of molecular assemblies in which a chromophore is linked to both an electron acceptor and an electron donor. These systems have been shown to generate relatively long lived photoinduced charge-separated states.[1-6]

We have recently reported time-resolved emission studies on donor-chromophore-acceptor (D-C-A) molecular assemblies which exhibit intramolecular charge separation.[7] These systems are based on a substituted ruthenium(II) trisbipyridine ($Ru(bpy)_3^{2+}$) chromophore, covalently attached to a *N,N'*-diquaternary-2,2'-bipyridinium salt (diquat, DQ^{2+}) electron acceptor, and two phenothiazine (PTZ) electron donors. An example structure is shown in Figure 1. Irradiation produces a long-lived charge-separated (CS) state in which the PTZ is oxidized, the diquat is reduced, and the $Ru(bpy)_3^{2+}$ is returned to the ground state. This CS state has been observed previously using transient absorption spectroscopy 50 ns after excitation of the complex.[2]

Our earlier emission studies have partially elucidated one mechanism by which this CS state is formed in these D-C-A complexes.[7] The chromophore, $Ru(bpy)_3^{2+}$, absorbs visible light and is excited into its metal-to-ligand charge transfer (MLCT) state. The excited species, $Ru(bpy)_3^{2+*}$, is best described as $Ru^{III}(bpy)_2(bpy^{\bullet-})^{2+}$, in which a d-electron from the metal has been moved to a π-orbital localized on one of the bipyridines. In this excited state, $Ru(bpy)_3^{2+*}$ is both a stronger reducing agent and a stronger oxidizing agent than it is in the ground state; consequently it is subject to either oxidative or reductive quenching of the MLCT emission. When an electron acceptor is present, the unpaired electron of $bpy^{\bullet-}$ can be transferred to the acceptor, reducing it. In the presence of a donor, an electron is transferred from the donor to the unoccupied metal d-orbital, thereby oxidizing the donor. Comparison of the electron transfer rates from the MLCT state for analogous chromophore-acceptor and donor-chromophore-acceptor complexes has shown that the initial electron transfer step, in all cases, is from $bpy^{\bullet-}$ to diquat.[7] Donor-to-chromophore electron transfer occurs only following oxidative quenching. In the case of an intramolecular assembly containing an acceptor and a donor, these sequential charge transfer reactions occur resulting in a charge-separated state in which the donor is oxidized, the acceptor is reduced, and the ruthenium chromophore is returned to its initial ground state, $Ru(bpy)_3^{2+}$.

Previous studies have also shown that the quantum yield for formation of the charge-separated state is quite solvent dependent. This result is interpreted in terms of the competition between reverse (acceptor-to-chromophore) electron transfer (ET) and donor-to-chromophore electron transfer. We suggested that, due to the electrostatic work term, the reverse ET rate is strongly dependent on the dielectric properties of the solvent, but the (uncharged) donor-to-chromophore ET rate is not.

Our approach to further understanding the formation of the charge-separated states in these systems is to determine the appearance kinetics of the oxidized donor (PTZ^+) and reduced acceptor (DQ^+) species within a series of D-C-A complexes. The D-C-A complexes studied here have the general form $[Ru(44\text{-}PTZ)_2(4mn\text{-}DQ^{2+})]^{4+}$. 44-PTZ is a phenothiazine containing ligand, 4-methyl-4'-(4-(*N*-phenothiazinato)butyl)-2,2'-bipyridine. The electron accepting ligand consists of a bipyridine moiety which is methylated at the 4-position, linked at the 4'-position via a methylene chain (length, *m*) to a diquat. The pyridinium nitrogens of the diquat are linked by a methylene chain of length *n*. In this work, *m* is always 2, and *n* is either 2, 3, or 4. Thus, ruthenium complexes containing two 44-PTZ ligands and either a 422-DQ^{2+}, a 423-DQ^{2+} (Figure 1), or a 424-DQ^{2+} ligand were studied.

The results presented here show that in all solvents the first step in charge separation from the MLCT state is oxidative quenching by the acceptor. In low-polarity solvents, once an electron is transferred from Ru^{2+*} to DQ^{2+}, ET from PTZ to Ru^{III} is quite fast and can compete with reverse electron transfer. Another very fast process was also found to contribute to the formation of the charge-separated state. These two mechanisms,

* Authors to whom correspondence should be addressed.
† Current Address: Department of Chemistry, Physical Sciences Building, Rhode Island College, Providence, RI 02908.

(1) *Photoinduced Electron Transfer*; Fox, M. A., Chanon, M., Eds.; Elsevier: Amsterdam, 1988; and text and references therein.
(2) Danielson, E.; Elliott, C. M.; Merkert, J. W.; Meyer, T. J. *J. Am. Chem. Soc.* **1987**, *109*, 2519.
(3) Wasielewski, M. R.; Niemczyk, M. P.; Svek, W. A.; Pewitt, E. B. *J. Am. Chem. Soc.* **1985**, *107*, 5562.
(4) Nishitani, S.; Kurata, N.; Sokata, Y.; Misumi, S.; Karen, A.; Okada, T.; Mataga, N. *J. Am. Chem. Soc.* **1983**, *105*, 7771.
(5) Cowan, J. A.; Sanders, J.; Beddard, G. S.; Harrison, R. J. *J. Chem. Soc., Chem. Commun.* **1987**, 55.
(6) Gust, D.; Moore, T. A. *Science* **1989**, *244*, 35.
(7) Cooley, L. F.; Larson, S. L.; Elliott, C. M.; Kelley, D. F. *J. Phys. Chem.* **1991**, *95*, 10694.

0002-7863/92/1514-9504$03.00/0

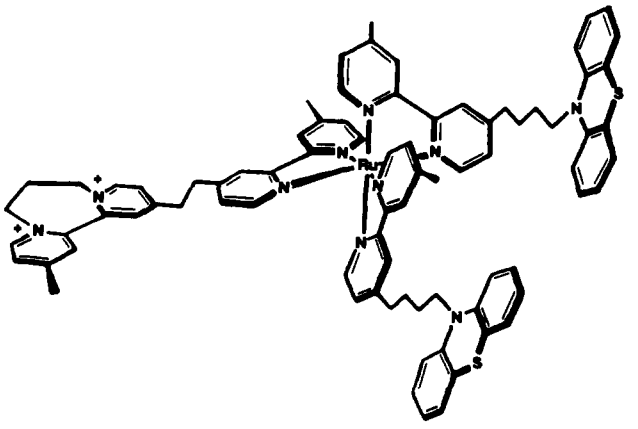

Figure 1. $[Ru(44\text{-}PTZ)_2(423\text{-}DQ^{2+})]^{4+}$.

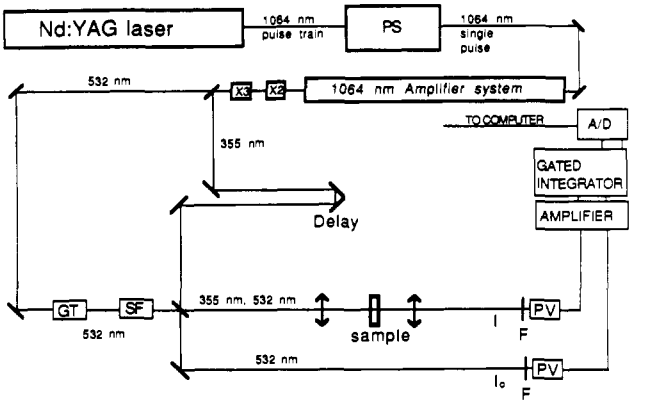

Figure 2. Schematic diagram of the time-resolved absorption apparatus. The following abbreviations have been used: PS, pulse selector; GT, Glan-Taylor polarizer; SF, spacial filter; F, filter (532 pass, 355 cut); PV, photovoltaic.

giving rise to the charge-separated state on two different time scales, provide an internal reference for studying the rates of reverse ET.

Experimental Section

Measurements. All electrochemical measurements were carried out in O_2-free, nitrogen-purged acetonitrile solutions with 0.1 M tetra-*n*-butylammonium hexafluorophosphate ($TBAPF_6$) as supporting electrolyte. A conventional three-electrode cell was used with a glassy carbon working electrode, a platinum wire loop auxiliary electrode, and a saturated calomel electrode (SCE) as reference.

Cyclic voltammetry was performed on a PAR Model 173 potentiostat.

Materials. All reagents and solvents were purchased commercially and used without further purification except as noted. $TBAPF_6$ was prepared as previously reported,[8] recrystallized three times from hot ethanol, and dried under vacuum. 4,4′-Dimethyl-2,2′-bipyridine (DMB) was recrystallized from ethyl acetate before use.

The eluent for thin layer chromatography (TLC) was a 50% acetonitrile, 40% water, and 10% saturated aqueous KNO_3 solution (by volume).

The preparations of all $42n\text{-}DQ^{2+}$ ligands and all ruthenium trisbipyridine complexes considered here have been reported previously.[9,10]

Picosecond Kinetic Measurements. The apparatus used for the time-resolved absorption measurements is shown in Figure 2. The system is based on an active/passive mode-locked Nd-YAG laser with a single pulse selector and amplifier system. Samples were excited with the third harmonic, 355- or 460-nm-light (30 ps, 60–70 μJ) pulses focussed to a spot size of ca. 1 mm. The sample was probed with second harmonic,

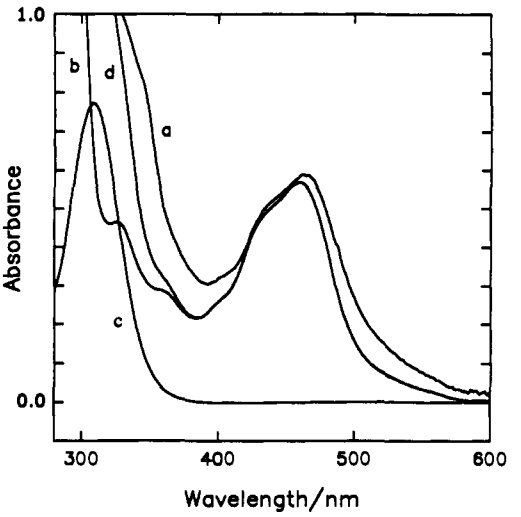

Figure 3. Electronic absorption spectra in 1,2-dichloroethane for (a) $[Ru(44\text{-}PTZ)_2(423\text{-}DQ^{2+})]^{4+}$, (b) $[Ru(DMB)_2(423\text{-}DQ^{2+})]^{4+}$, and (c) *N*-methylphenothiazine and (d) spectrum b plus spectrum c.

532-nm-light (30 ps, <5 μJ) pulses, collinear with the excitation pulses. The excitation and probe beam polarizations were placed at the magic angle (57.4°) to one another. A stepper motor driven variable delay controlled the relative arrival times of the excitation and probe pulses. The arrival time of the probe pulse could be varied from −1 to 12 ns, relative to the arrival of the excitation pulse. The temporal instrument response function was determined by convolution of the two 30-ps excitation and probe pulses, and is ca. 45 ps fwhm. The excitation beam was separated from the probe beam through the use of Hoya Y48 and Y50 filters. Two beams, a probe and a reference, were collected on two EGG UV-100-BQ photovoltaics. The output of each photovoltaic was amplified, integrated, and digitized on each laser shot. Digitized signals were stored in an IBM PC/AT computer, which also controls firing of the laser and movement of the delay stage. In some experiments, anti-stokes Raman shifting of the 532-nm second harmonic in a high-pressure methane cell was used to provide 460-nm excitation light.

The magnitude of the transient absorption signal depends on the sample concentration and on alignment of the pump and probe beams at the sample as well as the extinction coefficients for the various transitions. Since the alignment of the two beams is impossible to reproduce exactly from day to day, it is not possible to compare the intensities of spectra. Absolute transient absorbances varied from 0.04 to 0.2 depending on the above variables.

Preparation of Samples for Kinetic Studies. Solid samples of all the complexes were either kept rigorously in the dark or stored in a drybox (Vacuum Atmospheres Corp.) under N_2 atmosphere to prevent photodecomposition in the presence of O_2. Samples were prepared in the drybox. A small quantity (ca. 2 mg) was transferred to a sample tube, consisting of a 2 mm path length quartz cell attached to a Pyrex tube sealed with a Kontes Teflon-and-glass valve. Sample tubes were then sealed in the drybox, wrapped in aluminum foil, removed from the drybox, placed on a vacuum line outside the drybox, and evacuated for about 5 min ($<5 \times 10^{-3}$ Torr). A portion of the desired solvent (dichloroethane, Aldrich reagent grade; acetonitrile, J.T. Baker Photorex; both were used without further purification) was then degassed by 3–4 cycles of freeze–pump–thaw and distilled over to a Pyrex sidearm of the sample cell. Two more freeze–pump–thaw cycles were then performed, and the sample tubes were sealed under vacuum. Sample absorbances generally ranged from 0.2 to 0.8 at 290 nm.

Results

The static absorption spectrum of the D–C–A complex $[Ru(44\text{-}PTZ)_2(423DQ^{2+})]^{4+}$ is shown in Figure 3. Also shown in Figure 3 are the absorption spectra of $[Ru(DMB)_2(423\text{-}DQ^{2+})]^{4+}$ (DMB ≡ 4,4′-dimethylbipyridine) and *N*-methylphenothiazine (Me-PTZ). These spectra are scaled to correspond to 2 equiv of Me-PTZ per equiv of $[Ru(DMB)_2(423\text{-}DQ^{2+})]^{4+}$. Thus, the sum of the Me-PTZ and the $[Ru(DMB)_2423\text{-}DQ^{2+}]^{4+}$ spectra (also shown in Figure 3) corresponds to the individual chromophores in the D–C–A complex, $[Ru(44\text{-}PTZ)_2(423\text{-}DQ^{2+})]^{4+}$. It is of interest to compare the $[Ru(DMB)_2(423\text{-}DQ^{2+})]^{4+}$ and Me-PTZ summation spectrum with the spectrum of the D–C–A complex. While the two spectra show roughly comparable intensities at 460

(8) Sawyer, D. T.; Roberts, J. L. *Experimental Electrochemistry for Chemists*; Wiley: New York, 1974.
(9) Elliott, C. M.; Freitag, R. A.; Blaney, D. D. *J. Am. Chem. Soc.* **1985**, *107*, 4647.
(10) Cooley, L. F.; Headford, C. E. L.; Elliott, C. M.; Kelley, D. F. *J. Am. Chem. Soc.* **1988**, *110*, 6673.

Table I

complex	magnitude: slow rise (A)	magnitude: fast rise (A_f)	slow rise time (ps)	emission decay time (ps)*	A_f/A_s	k_{rev}/k_2	quantum yield[a]
$[Ru(44\text{-}PTZ)_2(422\text{-}DQ^{2+})]^{4+}$	0.197	0.803	150	240	4.08	8.85	0.10
$[Ru(44\text{-}PTZ)_2(423\text{-}DQ^{2+})]^{4+}$	0.38	0.62	820	960	1.6	2.85	0.26
$[Ru(44\text{-}PTZ)_2(424\text{-}DQ^{2+})]^{4+}$	0.49	0.51	3000	3120	1.0	1.40	0.42

[a] Quantum yields are calculated from relative values obtained from the A_f/A_s ratio assuming an absolute value for $[Ru(44\text{-}PTZ)_2(423\text{-}DQ^{2+})]^{4+}$ of 0.26 as determined in ref 2.

nm, the D–C–A complex shows greater absorption to the red of 460 nm and to the blue of 400 nm. For freshly synthesized and purified samples the absorption intensity to the red of 460 nm is greatly diminished relative to that of samples which have experienced greater exposure to atmospheric oxygen. In contrast, the increased absorption intensity (relative to spectrum d of Figure 3) appearing to the blue of 400 nm remains constant and is not a function of sample history. The absorption shoulder to the red of the MLCT transition thus appears to be due to a small concentration of a strongly absorbing impurity which is apparently generated by the unavoidable exposure of the sample solutions to O_2 during the chromatographic purification. Once samples are completely isolated from O_2 the static spectra do not change with exposure to light. The important point to be emphasized here, however, is that the concentration of this apparent impurity does not seem to affect the time-resolved results. Again, the enhanced absorption below 420 nm is independent of sample history. We assign this band to an interaction between the PTZ and $Ru(bpy)_3^{2+}$ chromophores in $[Ru(44\text{-}PTZ)_2(423\text{-}DQ^{2+})]^{4+}$. As expected, this band is absent in the nonbonded system. Due to the low PTZ ionization potential, this absorption can probably be assigned to a $PTZ/Ru(bpy)_3^{2+}$ charge transfer (CT) band. Figure 3 shows that a significant fraction (38%) of the D–C–A absorption at 355 nm is due to this charge transfer band. We note that the enhanced absorption below 420 nm is also present in these analogous D–C complexes, $[Ru(44\text{-}PTZ)_2DMB]^{2+}$. The majority of the band must therefore be assigned to $PTZ/Ru(bpy)_3^{2+}$ interaction, rather than PTZ/DQ^{2+} interaction.

Transient absorption kinetics were measured for the D–C–A complexes, $[Ru(44\text{-}PTZ)_2(42n\text{-}DQ^{2+})]^{4+}$ (n = 2, 3, 4), the donor–chromophore complex, $[Ru(44\text{-}PTZ)_2DMB]^{2+}$ and the chromophore–acceptor complex, $[Ru(DMB)_2(423\text{-}DQ^{2+})]^{4+}$. In all cases, the absorbance change was detected at 532 nm. This wavelength was chosen because both the oxidized phenothiazine moiety (PTZ^+) and the reduced diquat moiety (DQ^+) have significant 532-nm absorbances, while the ground state complex and the excited MLCT state do not. Consequently, in D–C–A complexes the transient absorption results at 532 nm directly give the kinetics of the charge-separated state. These kinetics were obtained in acetonitrile or dichlorethane (DCE) solvents, following excitation at 355 or 460 nm. The absorption results can be compared to previously reported emission decay times.[7]

In DCE solvent the $[Ru(44\text{-}PTZ)_2(42n\text{-}DQ^{2+})]^{4+}$ (n = 2, 3, 4) complexes each exhibit transient absorption behavior at 532 nm which is excitation wavelength dependent. Following 355-nm excitation the appearance of the absorption shows two kinetic components: a fast (pulse width limited) component and a slower component having the same time constant as the MLCT excited state decay. The transient absorption data for $[Ru(44\text{-}PTZ)_2(42n\text{-}DQ^{2+})]^{4+}$ (n = 2, 3, 4) following 355-nm excitation are shown in Figure 4, and the rate constants and relative contribution of the fast and slow components are given in Table I. Upon excitation at 460 nm qualitatively the same kinetics are observed except that the relative contribution of the fast component to the total absorbance is much smaller (≤15%). The appearance kinetics of the slow components are the same for both excitation wavelengths. In either case, following the slow rise, the 532-nm absorbance remains essentially constant on the time scale of a few nanoseconds. Preliminary transient absorption measurements in the nanosecond time regime indicate that each of the D–C–A complexes has a CS-state lifetime in the 100–200-ns range, which is consistent with previous published values for the 423-DQ^{2+}-containing analogue.[2] Thus, the CS state decays completely by the next laser shot (300 ms).

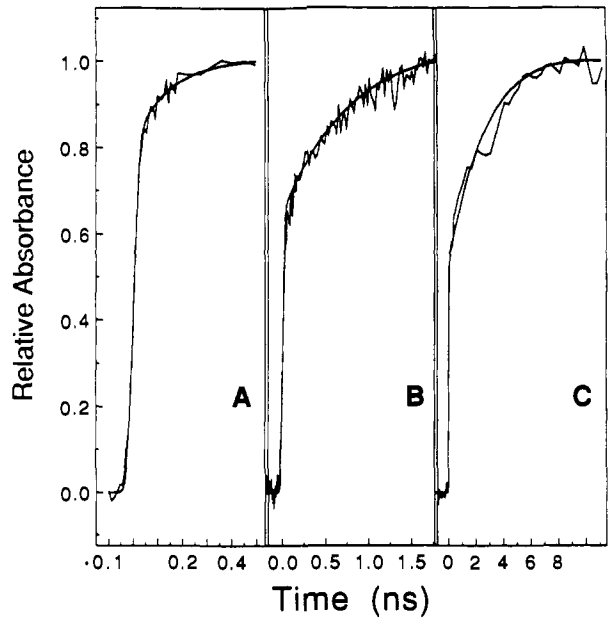

Figure 4. Transient absorption kinetics in 1,2-dichloroethane for $[Ru(44\text{-}PTZ)_2(42n\text{-}DQ^{2+})]^{4+}(PF_6^-)_4$: (A) n = 2, (b) n = 3, (C) n = 4. Shown with the experimental curves are best fits to a pulse width limited component plus a single exponential rise.

In acetonitrile solvent very simple 532-nm absorption kinetics are observed. Following 355-nm excitation only the fast, pulse width limited rise is observed. Following 460-nm excitation, no transient absorbance is detectable.

Following 355-nm excitation in both DCE and acetonitrile, $[Ru(44\text{-}PTZ)_2DMB]^{2+}$ shows only a fast rise in the 532-nm absorption. $[Ru(DMB)_2(423\text{-}DQ^{2+})]^{4+}$ shows no detectable transient absorbance (fast or slow) for either excitation wavelength. These observations are consistant with only the PTZ^+ and DQ^+ moieties having a significant 532-nm absorbance and the charge separation mechanism discussed below.

Finally, in transient absorption experiments where the sample is subjected to significant radiant power there is some reason for concern that chlorinated hydrocarbon solvents such as DCE might be reactive. We believe this not to be the case in the experiments reported here for two reasons. First, static absorption spectra of the solutions used for these experiments taken before and after multiple laser pulse irradiation are exactly superimposable over the wavelength range from 190 to 820 nm. Second, results of transient absorption experiments of the D–C–A complexes in 1,2-difluorobenzene solvent are qualitatively the same as those obtained in DCE. The greatly reduced potential reactivity of 1,2-difluorobenzene compared to DCE makes it unlikely that solvent chemical reactivity is participating in either case.

Discussion

The spectra and kinetics of the D–C–A complexes can be understood in terms of two mechanisms by which the charge-separated state is formed. One mechanism results in charge separation on the same time scale as the decay of the MLCT state; the other is a fast, pulse width limited process. Scheme I shows the two proposed mechanisms. In mechanism I, excitation results

Table II. Electrochemical Potentials for PTZ-Linked Complexes (vs SCE)

	Ru (3+/2+)	PTZ (1+/0)	DQ (2+/1+)	DQ (1+/0)	Ru (2+/1+)	Ru (1+/0)
$[Ru(44\text{-}PTZ)_2422\text{-}DQ^{2+}]^{4+}$	+1.14	+0.69	−0.43	−0.89	−1.43	−1.58
$[Ru(44\text{-}PTZ)_2423\text{-}DQ^{2+}]^{4+}$	+1.14	+0.70	−0.64	−0.86	−1.42	−1.59
$[Ru(44\text{-}PTZ)_2424\text{-}DQ^{2+}]^{4+}$	+1.12	+0.69	−0.77	−0.90	−1.40	−1.59

Scheme I. Two Mechanisms Giving Rise to Charge Separation in Dichloroethane

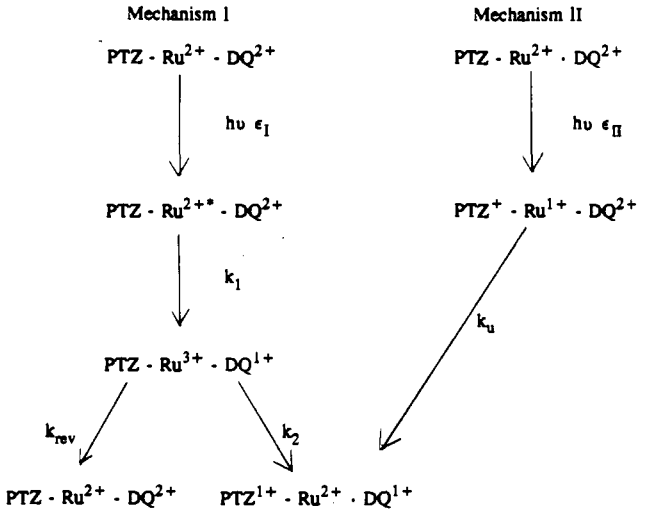

in population of the MLCT state. In this state, the optical electron is localized on one of the bipyridine moieties, which is linked to either a diquat or phenothiazine. Once interligand electron transfer has placed the electron on the bipyridine moiety which is linked to the diquat (the "adjacent" bipyridine), bipyridine-to-diquat electron transfer can occur. We have previously shown that bipyridine-to-diquat ET from the bipyridines which are linked to the PTZ's (the "remote" bipyridines) is slow compared to the former process.[10] The rates of interligand electron transfer (ILET) have recently been measured[11] and were found to be fast compared to bipyridine-to-diquat ET. Thus, MLCT quenching can be described by a single rate constant, denoted as k_1.

This rate constant was previously determined from emission decay measurements, which give the MLCT state lifetimes for the three D–C–A complexes studied. Following MLCT state quenching, a subsequent electron transfer must occur from the phenothiazine to the Ru^{3+} for the CS state to be formed. The rate of this electron transfer, denoted as k_2 in Scheme I, must compete with the reverse electron transfer from the DQ^{1+} to the Ru^{3+}, k_{rev}. The slowly rising component of the transient absorption curves can be fit to the corresponding MLCT state decay rate for all three complexes. This leads to the conclusion that $k_2 + k_{rev} \gg k_1$. Consistent with this conclusion, previous studies have shown that k_{rev} is at least an order of magnitude larger than k_1. If k_2 is at least comparable to k_{rev}, i.e., there is a significant quantum yield for CS state formation, then we also conclude that ET between the phenothiazine and the ruthenium occurs rapidly after the initial quenching of the MLCT state by the diquat. Since the slow rise mimics $1/k_1$ for all three complexes, this component of the transient is attributed to the formation of CS state via mechanism 1. Bipyridine-to-diquat ET is known to occur in acetonitrile from emission quenching.[10] Thus, the lack of any slowly rising component in acetonitrile indicates that $k_{rev} \gg k_2$ in this solvent. This result can be understood in terms of the comparison of acetonitrile and DCE solvent properties and has been discussed in a previous publication.[7]

The fast rising portion of the transient absorption can be understood in terms of mechanism II in Scheme I. In this mechanism, the first step is a photoinduced direct charge transfer between the phenothiazine and Ru^{2+}, forming oxidized phenothiazine and reduced ruthenium (Ru^{1+}). This process is followed by ET from the ruthenium to the diquat, forming the CS state. The spectra presented in Figure 3 imply that the transition responsible for this mechanism is a direct charge transfer (CT) process. This interpretation is further corroborated by transient absorption kinetics following 355- and 460-nm excitation. Figure 3 shows very little CT absorption at 460 nm. Correspondingly, when the excitation wavelength is 460 nm, very little of the fast component is observed.

In mechanism II, the oxidized phenothiazine is formed immediately upon photoexcitation, and the CS state is formed with a rate constant designated as k_u. Since both PTZ^+ and DQ^+ moieties absorb 532-nm light, some of the transient associated with this mechanism should appear immediately, and some should grow in with a rate of k_u. However, no kinetic component is observed which can be assigned to k_u; the appearance kinetics can be fit to an instrument limited rise (mechanism II) and a rise which matches the MLCT state decay (mechanism I). We therefore conclude that k_u^{-1} is less than about 20 ps and suggest that charge separation is fast because there is a large negative ΔG for formation of the charge-separated state.

It is of interest to compare the relative amplitudes of the fast and slow components in the different D–C–A complexes because this will allow the estimation of reverse ET rates. When excited at 355 nm, there is direct excitation to several states: the MLCT state, the bipyridine π,π^* state, the d–d state, and the $[PTZ\text{-}Ru(bpy)_3]^{2+}$ CT state. In all but the last case, the system quickly relaxes into the MLCT state. The magnitude of the fast component depends only on the CT extinction coefficient, assuming that absorption into the CT band produces the CS state with unit quantum efficiency. The extinction coefficient of the CT transition is expected to be independent of the type of acceptor moiety in the molecule ($422\text{-}DQ^{2+}$, $423\text{-}DQ^{2+}$, or $424\text{-}DQ^{2+}$) or, for that matter, the presence or absence of an acceptor. Furthermore, the transient absorption results from the D–C complexes show that the rate of $Ru(bpy)_3^+$-to-PTZ^+ electron transfer is slow, suggesting that absorption into the CT band produces the CS state with unit quantum efficiency. The one caveat to the above argument is the possibility that there is a rapid partitioning of the CT excited state population. In this case, some fraction of the CT excited molecules could undergo rapid Ru^+-to-PTZ^+ electron transfer while the rest form the CS state. The flexibility of the methylene chain connecting the PTZ to the $Ru(bpy)_3$ could conceivably cause this to occur. For example, it is possible that following CT excitation very rapid $PTZ^+ \rightarrow Ru(bpy)_3^+$ back ET would compete with separation of the PTZ^+ and $Ru(bpy)_3^+$ moieties and that only the latter process would lead to the CS state. This would result in a quantum yield for formation of the CS state which is less than unity. We emphasize that while this is possible there is no reason to believe that such a partitioning occurs, and it is likely that the magnitude of the fast component is the same and close to unity for the three D–C–A complexes.

The magnitude of the slow component varies with the relative values of k_2 and k_{rev} as indicated in mechanism I. The formation of the charge transfer state in mechanism I involves oxidation of the phenothiazine and reduction of the ruthenium which occurs with a rate of k_2. This process will be the same in all three complexes because the diquat remains reduced to DQ^+ and is therefore not involved. The value of k_{rev}, however, is affected by the diquat reduction potential (electrochemical potentials are given in Table II). The easier the DQ^{2+} is to reduce to DQ^{1+}, the harder it is to oxidize DQ^{1+} to DQ^{2+} in the reverse electron transfer process (k_{rev}). The magnitude of the slow component should vary with the ΔG for reverse electron transfer because reverse ET

(11) Cooley, L. F.; Bergquist, P.; Kelley, D. F. *J. Am. Chem. Soc.* **1990**, *112*, 2612. Malone, R. A.; Kelley, D. F. *J. Chem. Phys.* **1991**, *95*, 8970.

competes with formation of the CS state.

The presence of the fast component following 355-nm excitation allows the determination of the k_{rev}/k_2 ratio as a function of ΔG. The curves shown in Figure 4 indicate that the magnitude of the slow component decreases on going from $[Ru(44\text{-}PTZ)_2(424\text{-}DQ^{2+})]^{4+}$, to 423, to 422, assuming the magnitude of the fast component is constant. The value k_{rev} is thus smallest in the 424 complex.

The free energies for reverse electron transfer can be estimated from the electrochemical redox potentials. Table II shows the redox potentials for the three donor–chromophore–acceptor complexes. Formation of the CS state following oxidative quenching of the ruthenium by the diquat requires one-electron oxidation of the phenothiazine to 1+, which has a driving force of −0.44 V for each of the complexes. The reverse electron transfer for the three complexes involves reduction of the ruthenium from 3+ to 2+ (1.14 V) and oxidation of the diquat from 1+ to 2+ (−0.77, −0.64, and −0.43 V for the 424, 423, and 422 complexes, respectively). So the driving force for formation of the charge-separated state is −0.44 V while the driving force for the back electron transfer is −1.90, −1.78, and −1.57 for the 424, 423, and 422 complexes, respectively. Apparently, the rate of reverse electron transfer is largest when the driving force is smallest, placing reverse electron transfer in the Marcus inverted region.[12] ΔG for reverse electron transfer varies from −1.5 to −1.9 V. These values are large enough to make the above conclusion plausible.

Comparison of the two mechanisms (Scheme I) giving rise to the CS state yields quantitative estimates of how k_{rev} varies with ΔG. An expression for the magnitude of the slow component is given by

$$A_s = \epsilon_I \Phi_{cs} = \epsilon_I [k_2/(k_{rev} + k_2)]$$

where ϵ_I is the extinction coefficient for MLCT excitation. The amplitude of the fast component is simply proportioned to ϵ_{II}. The ratio of the two amplitudes is given by

$$A_s/A_f = (\epsilon_I/\epsilon_{II})[k_2/(k_2 + k_{rev})]$$

or

$$\begin{aligned} A_f/A_s &= (\epsilon_{II}/\epsilon_I)[(k_2 + k_{rev})/k_2] \\ &= (\epsilon_{II}/\epsilon_I)[1 + (k_{rev}/k_2)] \end{aligned} \quad (1)$$

Thus, relative values of k_{rev} can be determined from the ratios of slow to fast components.

Determination of the quantity $k_2/(k_2 + k_{rev})$ requires knowledge of ϵ_{II}/ϵ_I. From the spectra in Figure 3, a value for ϵ_{II}/ϵ_I of about 0.65 is obtained. Using eq 1 above, and the value for A_f/A_s for the 423 complex given in Table I as 1.6, $\Phi_{cs}(423)$ is calculated to be 0.42. Again, the above discussion assumes that excitation of the CT band produces the CS state with unit quantum efficiency. Lowering this assumed quantum efficiency lowers the calculated value of $\Phi_{cs}(423)$; thus, the calculated value of 0.42 is an upper limit on Φ_{cs}. Meyer, Elliott, and co-workers previously obtained the value of 0.26 for the quantum yield in the 423 complex in dichloromethane.[2] Assuming that the kinetic behavior is the same in dichloromethane as in DCE, it follows that $k_2/(k_2 + k_{rev}(423)) = 0.26$, which is in reasonable agreement with the value obtained from the transient and static spectra. With use of the observed ratios of fast to slow components for the 422 and 424 complexes (Table I), the above procedure also gives the values for A_f/A_s, Φ_{cs}, and k_{rev}/k_2 for these complexes (also given in Table I).

The observed variation of reverse ET rates with driving force cannot be adequately explained by classical Marcus theory.[12] An attempt to interpret these results in terms of classical Marcus theory leads to contradictions with the forward ET rates, as explained below.

The reverse ET rate is given by

$$k_{rev} = A \exp(-\Delta G^{\ddagger}/RT)$$

where A is a constant which will be taken to be the same for the 422, 423, and 424 D–C–A complexes. The value of $\Delta G^{\ddagger}$ is given by Marcus theory

$$\Delta G^{\ddagger} = \frac{\lambda}{4}\left(1 + \frac{\Delta G}{\lambda}\right)^2$$

where ΔG is the reaction exothermicity and λ is the reorganization energy. A value of λ can be estimated from a comparison of, for example, the 422 and 424 complex reverse ET rates. In this case

$$\begin{aligned} RT \ln (k_{422}/k_{424}) &= (\Delta G^{\ddagger}_{422} - \Delta G^{\ddagger}_{424}) = \\ &(\Delta G_{422} - \Delta G_{424})/2 + (\Delta G_{422}^2 - \Delta G_{424}^2)/4\lambda \end{aligned} \quad (2)$$

By solving eq 2 and using the rates from Table I and the appropriate exothermicities (Table II), a λ value of 1.36 V is calculated. This value can be compared to the λ value of about 800 mV as determined for the forward (bpy^{-} to DQ^{2+}) ET reaction.[10] Because changes in the magnitude of the dipole are about the same, the forward and reverse ET reactions are expected to have roughly comparable outer-sphere contributions to the reorganization energy. The inner-sphere contributions to the barriers from very low frequency vibrational motions are also expected to be comparable. Thus, reorganization energies for the forward and reverse reactions are expected to be comparable, in contradiction to the observed result. Alternatively, by using the 800-mV value from the forward ET results, the ratio of reverse ET rates (k_{422}/k_{424}) can be calculated. The (k_{422}/k_{424}) ratio is calculated to be $>10^3$, in sharp contradiction with the ratio of $\sim$6.3 obtained from the results in Table I.

The relative reverse ET rates can be understood in terms of the role that high-frequency quantized vibrational modes play in highly exothermic ET processes. These modes act as energy acceptors in the ET process, much as they do in other forms of radiationless decay. This idea has recently been used to analyze reverse ET rates in related systems which also exhibit Marcus inverted behavior.[13] This treatment makes several quite reasonable assumptions about the ET process. These assumptions include the following: (1) the energy accepting "receiving" modes can be grouped together and treated as a single harmonic oscillator with a quantum spacing of $\hbar\omega_M$; (2) the ET is only weakly coupled to the receiving vibrational modes; and (3) low-frequency solute vibrations play a relatively minor role in the ET process. With these assumptions and approximations, the reverse ET rate is given by[13]

$$\ln (k_{rev}) \propto -\frac{\gamma \Delta G}{\hbar\omega_M} + \text{(other terms which vary only weakly with } \Delta G) \quad (3)$$

where

$$\gamma = \ln\left(\frac{\Delta G}{S_M \hbar\omega_M}\right) - 1$$

ΔG is the exothermicity of the reaction, and S_M is the electron-vibration coupling. The quantities S_M and ω_M are given by

$$S_M = \sum_j S_j$$

$$\omega_M = \sum S_j\omega_j/S_m$$

$$S_j = \tfrac{1}{2}(M_j\omega_j/\hbar)(\Delta Q_{eq,j})^2$$

where the index j refers to the jth accepting mode, with effective

(12) (a) Marcus, R. A. *J. Chem. Phys.* **1965**, *43*, 379–701. (b) Marcus, R. A. *Annu. Rev. Phys. Chem.* **1964**, *15*, 155. (c) Marcus, R. A. *J. Chem. Phys.* **1965**, *43*, 679.

(13) Chen, P.; Duesing, R.; Graff, D. K.; Meyer, T. J. *J. Phys. Chem.* **1991**, *95*, 5850 and references therein.

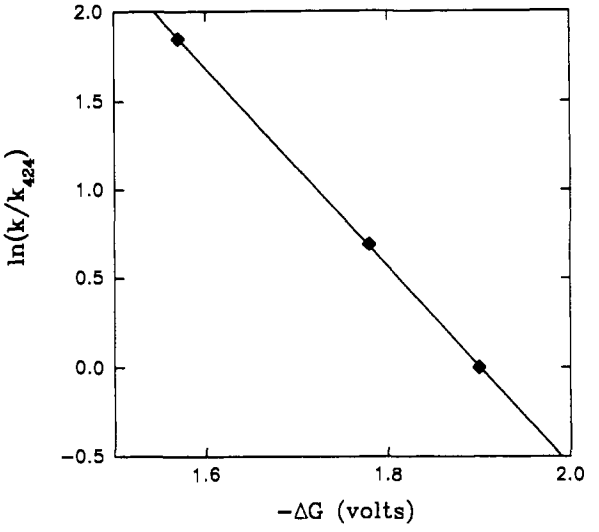

Figure 5. Plot of ln (k_{rev}) versus the reverse electron transfer driving force (ΔG) for $[Ru(44\text{-}PTZ)_2(42n\text{-}DQ^{2+})]^{4+}(PF_6^-)_4$ (n = 2, 3, 4).

mass M_j and frequency ω_j. $\Delta Q_{eq,j}$ is the ET induced equilibrium displacement along the jth mode. Thus, S_m is related to the activity of the receiving modes in the ET process.

Equation 3 predicts that the plot of ln (k_{rev}) vs ΔG will be approximately linear and have a slope of $-\gamma/\hbar\omega$. Such a plot is shown in Figure 5, and a linear relationship is obtained with a slope of about 5.0 eV^{-1}.

It is of interest to compare these results to the reverse ET rates reported by Mallouk et al.[14] for closely related C–A complexes in which Marcus inverted behavior is observed in the reverse ET rates. These complexes are the same as the C–A complexes described above, except the diquat moiety is replaced by a viologen. This slightly decreases the reverse ET driving force. Time-resolved studies show that both forward and reverse ET rates are much slower than in our case. However, the plot at ln k_{rev} vs $-\Delta G$ is approximately linear, and shows essentially the same slope (~5 eV^{-1}) as we observe.

We may also compare our results to those reported by Meyer et al.[13] for the series of compounds $[4,4'\text{-}X_2\text{-bpy})Re(CO)_3py\text{-}PTZ]^+$ (X = OCH_3, CH_3, H, $CONEt_2$, CO_2Et), in which Marcus inverted behavior is observed. For these systems, the reverse ET is from $4,4'\text{-}X_2\text{-bpy}^{\bullet-}$ to $PTZ^{\bullet+}$, and the ΔG values are of comparable magnitude to the system under consideration here. Although the reverse ET rates are much slower than in our case, the plot of ln (k_{rev}) vs ΔG exhibits a similar value of the slope (3.4 eV^{-1}).

A similar comparison may also be made to reverse ET in $[4,4'\text{-}X_2\text{-bpy})Re(CO)_3(dimethylaminobenzoate)]^+$, which recently has been studied by MacQueen and Schanze.[15] In this case the reverse ET is from the bipyridine$^{\bullet-}$ to dimethylaminobenzoate$^{\bullet+}$. This system is similar to that reported by Meyer et al., and the reverse ET rates show a very similar dependence on ΔG.

In all cases (the results reported here, and the three other studies mentioned above), roughly similar dependencies on the reverse ET rates on ΔG are observed. This is not surprising and follows from eq 3. In all cases the reverse ET involves oxidation or reduction of an aromatic moiety. Thus, the receiving modes involve C–C and C–N stretches and have comparable values of the electron-vibration coupling and acceptor mode frequencies. We note, however, that the actual reverse ET rates reported here are orders of magnitude faster than in the literature results discussed above. We conclude that despite the chemical differences between these systems (which can result in vastly different electronic coupling) the extent of electron-vibration coupling and acceptor mode frequencies are roughly comparable.

Summary and Conclusions

Transient absorption of the charge-separated state in a donor–chromophore–acceptor complex is seen to arise by two separate mechanisms. A charge transfer transition is thought to be responsible for a fast rise in transient absorbance while a transition to the MLCT state of $Ru(bpy)_3^{2+}$, quenching by the diquat acceptor, and fast oxidation of the phenothiazine donor moiety are responsible for the slow component. The fast component is wavelength dependent and identical for the three complexes studied, thus providing an internal reference for measuring the magnitude of the slow component.

The magnitude of this slow component is dependent on the competition between oxidization of the donor and reverse electron transfer. The rate of reverse electron transfer is seen to vary with driving force in the opposite manner to that predicted by normal Marcus behavior. This is interpreted as evidence of Marcus inverted behavior in these intramolecular donor–chromophore–acceptor complexes. The results can be understood in terms of the involvement of high-frequency quantized modes in the reverse ET process.

Acknowledgment. This work was supported by grants from NSF [CHE-8821752 (C.M.E.) and CHE-8814351 (D.F.K.)] and the donors of the Petroleum Research Fund, administered by the American Chemical Society (D.F.K.). We also thank Professor Tom Mallouk for providing a preprint of ref 14.

Registry No. MePTZ, 1207-72-3; $[Ru(44PTZ)_2(422\text{-}DQ^{2+})]^{4+}$, 136847-78-4; $[Ru(44PTZ)_2(423\text{-}DQ^{2+})]^{4+}$, 106763-61-5; $[Ru(44PTZ)_2(424\text{-}DQ^{2+})]^{4+}$, 136847-80-8; $[Ru(DMB)_2(423\text{-}DQ^{2+})]^{4+}$, 96897-20-0; $[Ru(44PTZ)_2DMB]^{2+}$, 143294-78-4.

(14) Yonemoto, E. H.; Riley, R. L.; Kim, Y. I.; Atherton, S. J.; Schmehl, R. H.; Mallouk, T. E. *J. Am. Chem. Soc.*, submitted for publication.

(15) MacQueen, D. B.; Schanze, K. S. *J. Am. Chem. Soc.* **1991**, *113*, 7470.